CoCr wear particles generated from CoCr alloy metal-on-metal hip replacements, and cobalt ions stimulate apoptosis and expression of general toxicology-related genes in monocyte-like U937 cells

Olga M Posada[a,I,d], Denise Gilmour[c], Rothwelle J. Tate[b], and M. Helen Grant[a]

[a]Biomedical Engineering Department, University of Strathclyde, Wolfson Centre, Glasgow G4 0NW, UK.

[b]Strathclyde Institute for Pharmacy & Biomedical Sciences, University of Strathclyde, Glasgow G4 0RE, UK. r.j.tate@strath.ac.uk

[c]Pure and Applied Chemistry Department, University of Strathclyde, Thomas Graham Building, Glasgow G1 1XL, UK.

[d]Corresponding author: O.M.PosadaEstefan@leeds.ac.uk. TEL: +44 (0) 113 343 7747

[I] Current address: LICAMM laboratories, University of Leeds, Leeds LS2 9JT, UK

Abstract

Cobalt-chromium (CoCr) particles in the nanometre size range and their concomitant release of Co and Cr ions into the patients' circulation are produced by wear at the articulating surfaces of metal-on-metal (MoM) implants. This process is associated with inflammation, bone loss and implant loosening and led to the withdrawal from the market of the DePuy ASR^{TM} MoM hip replacements in 2010. Ions released from CoCr particles derived from a resurfacing implant *in vitro* and their subsequent cellular up-take were measured by ICP-MS. Moreover, the ability of such metal debris and Co ions to induce both apoptosis was evaluated with both FACS and immunoblotting. qRT-PCR was used to assess the effects on the expression of lymphotoxin alpha (LTA), BCL2-associated athanogene (BAG1), nitric oxide synthase 2 inducible (NOS2), FBJ murine osteosarcoma viral oncogene homolog (FOS), growth arrest and DNA-damage-inducible alpha (GADD45A). ICP-MS showed that the wear debris released significant ($p<0.05$) amounts of Co and Cr ions into the culture medium, and significant ($p<0.05$) cellular uptake of both ions. There was also an increase ($p<0.05$) in apoptosis after 48h exposure to wear debris. Analysis of qRT-PCR results found significant up-regulation ($p<0.05$) particularly of NOS2 and BAG1 in Co pre-treated cells which were subsequently exposed to Co ions+debris. Metal debris was more effective as an inducer of apoptosis and gene expression when cells had been pre-treated with Co ions. This suggests that if a patient receives sequential bilateral CoCr implants, the second implant may be more likely to produce adverse effects than the first one.

Keywords: CoCr wear debris, Co ions; metal-on-metal hip replacements; apoptosis; toxicology gene expression.

Introduction

Despite improvements in implant design and surgical techniques, periprosthetic osteolysis causing aseptic loosening of artificial joints is still a complication limiting clinical success of total joint arthroplasty as the treatment of joint diseases (1, 2). When a hip replacement fails revision surgery may need to be performed. This causes morbidity risk for the patient (3) and, as the peri-implant tissue has been sensitised, the replacement implant may have an increased chance of failing. Particulate wear debris generated from the implants can provoke biological tissue responses, including vascularized granulomatous tissue formation along the implant-to-bone interface, inflammatory cell (macrophages, lymphocytes) influx, bone resorption,

osteolysis, and finally loss of prosthesis fixation (4). As part of the foreign body response to implants, macrophages are the cells that provide surveillance and coordinate the inflammatory cascade leading to wound healing and implant stability (2). The presence of wear debris in the peri-implant area leads to phagocytosis of particulate debris by macrophages and activation of these cells stimulates the release of a variety of mediators, such as free radicals and nitric oxide, as well as bone resorbing mediators such as interleukin-1 (IL-1), tumour necrosis factor-α (TNF-α), prostaglandin E2 (PGE2) and IL-6 (1). Additionally, Metals debris and metal ions can activate the immune system by inducing a delayed type IV hypersensitivity reaction (5). The most common sensitizing orthopaedic metals are nickel, cobalt, and chromium (5, 6). It is thought that the stimulated T-cells generate pro-osteoclastogenetic factors that can alter bone homeostasis (7) and therefore contribute to osteolysis. The prevalence of metal sensitivity among the general population is approximately 10% to 15% and the prevalence of metal sensitivity among patients with well-functioning and poorly functioning implants has been reported to be ~25% and 60%, respectively, as measured by dermal patch testing (5). The response of metal-specific lymphocytes has been linked to poor implant performance. Cell-mediated type-IV hypersensitivity reaction characterized by vasculitis with perivascular and intramural lymphocytic infiltration of the postcapillary venules, swelling of the vascular endothelium, recurrent localized bleeding, and necrosis has been reported following metal-on-metal hip replacements (8).

During revision surgeries or postmortem examination, discoloured tissue is frequently observed around CoCr implants; some patients feel unexplained pain that may be associated with the tissue damage caused by MoM hip replacement wear (3). Elevated levels of Co and Cr ions occur in the peripheral blood and in the hip synovial fluid after CoCr alloy metal-on-metal (MoM) hip replacement, and there is concern also about the toxicity and biological effects of such ions both locally and systemically (9, 10). The Medicines and Healthcare Products Regulatory Authority (MHRA) have suggested that combined whole blood Co and Cr levels of greater than 7ppb (7µg/l or 0.1µM) are associated with significant soft tissue reactions and failed hip implants.

Co ions and nanoparticles are cytotoxic and induce apoptosis, and at higher concentrations, necrosis, with inflammatory responses (11). It has been demonstrated that macrophage mortality induced by metal ions depends on the type and concentration of metal ions as well

as the duration of the exposure (12). Cobalt corrodes faster than chromium under physiological conditions (13) and, opposite to Cr, Co ions tend to remain mobile, which is reflected in the higher levels measured in blood, allowing them to reach remote organs (14). Elevated Co concentrations in patients with MoM implants are a concern, since increased cobalt levels in blood have also been reported to be associated with neurological (hand tremor, incoordination, cognitive decline, depression, vertigo, hearing loss, and visual changes) (15, 16) cardiac (myocardiopathy) (17) and endocrine (16) symptoms.

Over the past few years, a number of investigations have been carried out to study the effects of metal ions and particulate wear debris on the expression of an array of genes *in vitro*. However, to the authors' knowledge, the expression of human toxicology related genes such as lymphotoxin alpha (LTA), BCL2-associated athanogene (BAG1), growth arrest and DNA-damage-inducible alpha (GADD45A) and FBJ murine osteosarcoma viral oncogene homolog (FOS) has not been studied in the context of prosthetic wear debris. Patients undergo chronic exposure to this wear debris so a time point of 120h was chosen in this study to investigate any longer term in vitro effects on gene expression in the cells.

LTA, a member of the TNF family, is an inflammatory mediator that influences multiple processes such as activation, proliferation, differentiation, and death induction in many different cell types (18). BAG1 is a multifunctional protein able to delay cell death by a synergistic action with BCL2 (19). The family of growth arrest and DNA damage (GADD) proteins is composed of five regulatory molecules that function primarily to protect cells and ensure survival by inducing cell cycle arrest, DNA repair or promoting apoptosis (20). The FOS gene family consists of 4 members: FOS, FOSB, FOSL1, and FOSL2. FOS is a critical factor involved in osteoclast development and activation (21). Moreover, a pivotal role of FOS in nitric oxide synthase 2 (NOS2) expression in airway epithelial cells has been suggested (22). NOS2 is widely expressed in every type of tissue and cell after transcriptional induction following exposure to a vast array of immunologic and inflammatory stimuli (23).

In this study, ions released from CoCr particles derived from a resurfacing implant as well as their subsequent cellular up-take were measured by inductively coupled plasma mass spectrometry (ICP-MS). Moreover, the ability of the metal debris and cobalt (Co) ions to induce both apoptosis and general toxicology-related gene expression of human monocyte-like U937 cells was examined. In some experiments the cells were pre-treated with Co ions

prior to exposure to CoCr particles, in order to simulate the *in vivo* situation where a patient may receive a second MoM implant either a bilateral or a revision procedure. Co ion concentrations used in the present experiments were 0.1µM, reflecting the upper blood level threshold recommended by MHRA for patient safety. To the authors' knowledge, priming cells with metal ions for subsequent challenge with wear debris is a novel approach within this field and could developed into a viable cell culture model for analysis of the cellular effects of metal ions and particles.

Methods

Preparation of wear debris

CoCr wear debris was donated by DePuy International (Leeds, UK). A high-carbon cast cobalt chrome hip resurfacing implant was worn on a multi-station hip joint simulator over 250,000 cycles using distilled water as the lubricating fluid. The use of only distilled water (instead of the more usual bovine serum (25% (v/v) in distilled water) resulted in a more aggressive wear regime which produced a greater volume of wear debris of similar morphology and size to that produced under similar conditions in 25 per cent serum (C. Hardaker, DePuy International Ltd, Leeds, UK, personal communication). The wear debris suspended in distilled water was centrifuged at 3,500g for 20min. The water was then aspirated and the debris was heat-treated (180°C for 5h, 60kPa) in a vacuum oven to destroy any endotoxin. The dry debris was suspended in sterile phosphate buffered saline (PBS; Life Technologies; Paisley, UK). Heat-treated wear debris was characterised with a Field Emission Scanning Electron Microscope (FE-SEM) (Hitachi SU-6600, Hitachi; Germany) at magnifications of 100-1000x. The sample was then transferred to a Scanning Electron Microscope (SEM) (Hitachi TM-1000, Hitachi; Germany). Energy Dispersive X-ray Spectroscopy (EDS) was used for quantitative analysis of elemental composition. Hitachi TM-1000 and EDSwift-TM software was used to obtain the images and chemical spectra of the wear debris. The sterility of the treated wear debris was tested as described elsewhere (24) by exposing dendritic cells (isolated from bone marrow of male BALB/c (Harlan, UK) mouse femurs and tibias (25)) to the debris for 24h, *in vitro*, and assessing the expression of surface activation markers via flow cytometry. The debris was found not to increase the surface expression of CD40, CD86, or MHC II on these cells, and, therefore, the suspended debris was deemed sterile and endotoxin-free (data not shown).

Metal ion release into cell culture medium

2.5mg metal wear debris/1x10^6cells were incubated for 24h in RPMI-1640 (pH 7.4) in the presence and absence of foetal calf serum (FCS, Life technologies; Paisley, UK) and in complete RPMI-1640 at pH 4. Every condition was carried out in triplicate and controls of each condition with no metal debris were also present. In addition to this, 0.2, 0.5, 1, 2.5 and 5mg metal wear debris/1x10^6cells were incubated in complete RPMI-1640 for 24h at 37°C and 5% (v/v) CO_2. Every concentration was carried out in triplicate and appropriate controls with no metal debris were also present. At 24h, culture medium from each well was collected into microcentrifuge tubes and stored at -80°C until ICP-MS analysis.

Cell culture

U937 [Human leukemic monocyte lymphoma cell line; European Collection of Cell Cultures] cells were cultured in RPMI-1640 medium supplemented with 10% (v/v) FCS, 50U/ml penicillin and 50µg/ml streptomycin. Co^{2+} solutions were freshly prepared using cobalt chloride ($CoCl_2$) (Alfa Aesar; Lancashire, UK) and diluted to 0.1µM in growth medium under sterile conditions. In order to analyse ion up-take, resting cells were seeded at 1x10^5cells/ml in 24-well plates and exposed to 0, 0.2, 0.5, 1, 2.5 and 5mg metal wear debris/1x10^6cells for 24h at 37°C and 5% (v/v) CO_2. For cell viability assessment, cells were cultured (1x10^4cells/well) in 96-well plates with 5mg debris/1x10^6cells, 0.1µM of Co^{2+}, or the combination of 5mg debris/1x10^6cells plus 0.1µM of Co^{2+} in complete RPMI-1640 for 24 and 120h at 37°C under 5% (v/v) CO_2. For apoptosis analysis, 1x10^5cells/ml U937 cells and U937 cells treated with 0.1µM Co for 72h, were exposed for 24 and 48h (to measure both early apoptosis and detect any repair) to 2.5mg metal wear debris /1x10^6cells, 0.1µM Co and 2.5mg metal wear debris /1x10^6cells plus 0.1µM Co, in 12-well plates at 37°C and 5% (v/v) CO_2. For gene expression analysis, U937 and Co pre-treated U937 cells were exposed to the same three treatments but for a period of 120h. This longer time point was chosen to reflect the chronic effects of exposure to wear debris and ions on gene expression in patients *in vivo*.

ICP-MS analysis

For the analysis of cellular ion up-take, cells were centrifuged at 350xg for 5min, and then washed twice with PBS. After the second wash, the PBS was discarded and cell pellets sonicated for 30min at 45°C. Cell lysates were then resuspended in 1ml of ultrapure water (18mΩ) and stored at -20°C overnight. Thawed cell lysates and culture medium samples were centrifuged at 13,200rpm for 15min. Cell lysates were diluted 5-fold in 2% (v/v) HNO_3 and

culture medium samples were diluted 10-fold in RPMI-1640. Standards were prepared by diluting Multi-element Standard Solution 1 for ICP (Fluka) in 2% (v/v) HNO_3 (standards for cell lysates) or RPMI-1640 (standards for medium samples) for 1, 10, 50, 200, and 500µg/L Co final concentrations. All samples were analysed using an Agilent 7700x octopole collision system ICP-MS (Agilent Technologies; Wokingham, UK) in helium gas mode using Scandium as internal standard. The quantification was based on the maximum signal for a particular isotope, also referred to as peak height. Five readings were taken, and the result obtained was the mean value.

Cell viability measured by MTT

Culture plates were centrifuged at 350xg for 5min and supernatant aspirated. Cell pellets were suspended in 10mM 3-(4,5-dimethylthiazol-2-yl)-2,5-diphenyltetrazolium bromide (MTT; Sigma-Aldrich; Dorset, UK) solution (50µl) and then incubated for 4h at 37°C, under 5% (v/v) CO_2. Following incubation, culture plates were centrifuged (350xg, 5min) and supernatant removed. Cells were then resuspended in 200µl of dimethyl sulfoxide (DMSO) to dissolve the formazan product. Optical absorbance was measured at 540nm using a Bio-Rad Model 450 microplate reader (Bio-Rad, Hertfordshire, UK).

Cell viability measured by NR

Culture plates were centrifuged at 350xg for 5min and supernatant aspirated. Cell pellets were suspended in 0.2mM NR (Sigma-Aldrich; Dorset, UK) solution (100µl) and then incubated for 3h at 37°C, under 5% (v/v) CO_2. Following incubation, culture plates were centrifuged at 350xg for 5min and washed once with 200µl of PBS. NR de-stain solution was prepared by mixing together 50ml ethanol (Sigma-Aldrich; Dorset, UK), 1ml glacial acetic acid (Sigma-Aldrich; Dorset, UK) and 49ml distilled water. 100µl of this solution was added to each well and it was left for at least 30min on an orbital shaker until all of the pellets present had been dissolved and a homogeneous colour was obtained in each well. Optical absorbance was measured at 540nm using a Bio-Rad Model 450 microplate reader (Bio-Rad, Hertfordshire, UK).

Flow cytometry analysis of apoptosis

All buffers and stains for flow cytometry were obtained from BD Bioscience, Oxford, UK. At each endpoint, U937 cells were collected by centrifugation and washed twice with 100µl fluorescence-activated cell sorting (FACS) buffer (1×PBS containing 2% (v/v) FCS and

0.05% (w/v) sodium azide). Cells were then resuspended in 100µl 1×annexin binding buffer and incubated for 15min with aliquots (5µl) of phycoerythrin-labelled annexin V and 7-aminoactinomycin D in the dark. Thereafter, 200µl of 1×annexin binding buffer and FACS flow were added to each tube and the samples analysed by a FACSCanto flow cytometer (BD Bioscience). A minimum of 20,000 events in the target area were recorded for each sample. All data were analysed using FACSDiva software (BD Biosciences).

Western blot analysis of apoptosis

Total protein content was measured by Lowry assay (26). Homogenates from both treated and untreated U937 cells were prepared in Laemmli buffer and 10µg of protein were separated on 10% SDS-polyacrylamide gels (SDS-PAGE). Samples were immunoblotted using a rabbit polyclonal antibody to Poly-ADP-Ribose-Polymerase (PARP, 1:2000, Roche; West Sussex, UK) and anti-rabbit IgG-ALP (1:1000, BioRad; Hertfordshire, UK). The optical densities of the protein bands were then quantified using Image J 1.42q software.

RNA isolation and cDNA synthesis

Total RNA from cell cultures was extracted using the GenElute Mammalian Total RNA Miniprep Kit (Sigma-Aldrich; Dorset, UK) as described by the manufacturer, including the on-column RNase-free DNase digestion. RNA yield and purity were quantified by spectrophotometric analysis with NanoDrop 2000c (Thermo Scientific; Washington, USA). RNA integrity was verified with an Experion automated electrophoresis system (Bio-Rad; Hertfordshire, UK). cDNA was prepared from 4µg of total RNA using Superscript-II reverse transcriptase (Invitrogen; Paisley, UK) and oligo(dT)24 (500ng/µl, Eurofins MWG Operon; London, UK).

Quantitative Real-time PCR

Oligonucleotide primers (Table 1) for the genes of interest were used in SYBR-Green based quantitative real-time reverse-transcription-PCR on a StepOnePlus™ Real-Time PCR system (Applied Biosystems; Paisley, UK) with SYBR-Select Master Mix (Applied Biosystems; Paisley, UK). Primer sets were designed using the sequence analysis software, GeneRunner v3.05 (Hasting Software, USA) and Primer-BLAST (27) to produce an amplicon between 100 and 150bp long and to ensure the primers spanned exons to minimise the risk of genomic DNA amplification. Triplicate real-time PCR reactions were run with each primer set for each sample and contained 10µl SYBR-Select Master Mix, 3µl of forward primer (1pmol/µl;

Eurofins MWG Operon; London, UK), 3µl of reverse primer (1pmol/µl, Eurofins MWG Operon; London, UK), 1µl cDNA (33.3ng/µl) template, and molecular-grade H_2O (Sigma-Aldrich; Dorset, UK) up to the total reaction volume of 20µl. The following standard real-time PCR conditions were used: 1 cycle of 50°C for 2min; 1 cycle of 95°C for 2min; and 40 cycles of 95°C for 15s followed by 60°C for 1min. Following amplification, a melting curve analysis was performed to ensure the PCRs generated the single predicted amplicon. The StepOnePlus™ software (v2.1) automatically set the base line and threshold for each reaction. A quantification cycle (C_q) was assigned at the beginning of the logarithmic phase of PCR amplification and the difference in the C_q values of the control and experimental samples was used with the Comparative Cq method (28), to determine the relative expression of the gene in each sample. Template-negative controls were also run in order to test for genomic DNA contamination. Three genes (GAPDH, B2M, and HPRT1) were included as potential reference genes. After analysis of their expression stability under the treatment regimes using RefFinder (29) (data not shown), the gene HPRT1 was chosen as the reference gene and its expression used for normalization.

Statistics

Statistical analyses were carried out by a one-way analysis of variance, followed by a Dunnett's multiple comparison test and a two-sample *t*-test. Significance was assigned where *p* values were found to be <0.05.

Results

Characterisation of heat treated wear debris

SEM images show irregular shapes and sizes varying from the nano to the micro scale (from 150nm to 6.5µm). The larger irregular shaped particles suggest that the debris aggregates (Image 1), and this has been reported previously by Akbar and coworkers (24). EDS analysis indicated that the wear debris is primarily composed of Co and Cr, which is in agreement with the alloy composition (30). Analysis of 25 different particles indicated a mean composition of 59.57 per cent (± 1.15) Co and 40.43 (±1.25) per cent Cr, with a small content of Mo which was below the quantification limit.

Cell viability

U937 and Co pre-treated U937 cell viability was assessed after 24 and 120h of treatment in terms of metabolic activity (MTT) and cell number (NR) (Table 2). After 24h, there was a general increase in cell metabolic activity (MTT) in response to all treatments. In contrast to this, NR showed a significant decrease in cell number for Co pre-treated cells exposed to wear debris and the combination of wear debris and Co ions when compared to control untreated U937 cells. After 120h, there was significant decrease in both cell number (NR) and metabolic activity (MTT) where the debris was present. In contrast to this, a significant increase in both cell number (NR) and metabolic activity (MTT) was observed in cells treated with Co ions alone. In addition to the above, the effects on U937 and Co pre-treated U937 cells were compared in order to establish if the pre-treatment with Co ions made a difference to the effects caused by the exposure to metal debris and Co. At 24h, there was a significant difference caused by Co pre-treatment in the effect of 5mg debris/$1x10^6$cells in cell number. At 24h and 120h there was a significant difference caused by Co pre-treatment on the effects of combined 5mg debris/$1x10^6$cells and 0.1µM Co on cell number. These results suggest that chronic exposure to high concentrations of wear metal debris could have a detrimental effect on cell viability particularly if the cells have been previously exposed to Co ions.

Metal ion release into cell culture medium

Metal debris was incubated, in the absence of U937 cells, under different conditions in order to analyse the effects that some variables have on the amount of metal ions released into the culture medium. Analysis of ICP-MS results found that CoCr debris released metal ions into culture medium (Table 3). There was no significant difference ($p>0.05$) in ion release from metal debris in the presence and absence of 10% (v/v) FCS. This concentration of FCS was used as it was the concentration used when the CoCr wear debris was incubated with U937 cells for up to 120h to determine effects on apoptosis and gene expression. In contrast to these data, the acidic pH 4.0 had a considerable effect as seen in the significant increase ($p<0.05$) in the levels of ion release. Such a low pH was chosen in order to mimic local acidification during inflammation (31) and the acidic lysosomal medium (32). Even though Co was the ion predominantly released in all cases, the change in pH seemed to have a more pronounced effect on Cr ion release.

Increasing concentrations of metal debris were also incubated in order to analyse the correlation between debris concentration and metal ions released (Figure 1). Analysis of ICP-

MS results found a significant ($p<0.05$) increase in the amount of ions released with increasing wear debris concentrations. However, the increase in ion release was not linear with respect to debris concentrations (Figure 1). Once again, Co was the ion detected at the highest concentrations.

Metal ion up-take by U937 cells

U937 cells were exposed to increasing metal debris concentrations in order to establish cellular up-take of ions released into the culture medium by CoCr wear debris. Analysis of ICP-MS results found significantly higher ($p<0.05$) up-take of Co than Cr for all treatments (Figure 2, Table 4). Molybdenum (Mo) up-take into the cells could not be detected. There was an increase in ion up-take with increasing wear debris concentrations, but the increase in ion up-take was not linear with respect to debris concentrations. Additionally, a slight decrease was observed in ion levels measured when cells were exposed to 5mg debris/$1x10^6$cells probably due to the fact that this concentration has been shown to be cytotoxic. Of special interest is the fact that the Cr and Co ion concentrations in Figure 2 and Table 4 are expressed as concentration per single cell. This indicates that a significant high amount of metal ions was being taken up by the cells, and this could be related to the adverse tissue response to metal wear debris and ions. After their intracellular accumulation particles are often stored in acidic lysosomal vacuoles where intracellular dissolution can occur (32). As shown in the section above, significant increase in ion release was observed at pH 4. The results herein suggest that the levels of intracellular metal ions measured could be due to either intracellular ion release through the actions of the low pH compartments of the lysosomal-endosomal compartment following particle endocytosis or a combination of both intracellular particle degradation and ion up-take from the extracellular culture medium.

Apoptosis analysis

Cell viability assays carried out showed that the 5mg debris/$1x10^6$cells concentration was highly cytotoxic, and because of this 2.5mg debris/$1x10^6$cells concentration was chosen for the analysis of apoptosis and gene expression. Although this is still a high dose, it was considerably less toxic and allowed detection of early apoptosis, and isolation of enough RNA for the gene expression assays.

The results of examination of phosphatidylserine (PS) externalization and detection of the 89kD PARP fragment consistently revealed that CoCr wear debris induced apoptosis in U937

cells. Flow cytometry using Annexin V/FITC and 7-AAD double staining revealed that after exposure to 2.5mg debris/1x10^6cells and 2.5mg debris/1x10^6cells with 0.1µM Co, the number of cells with externalized PS started to increase by 24h of treatment. This increase became significant by 48h of exposure (Figure 3). Metal debris induced a greater PS externalization in cells that had been pre-treated with Co, as seen by the increase from 10.2%±0.4 early apoptosis in non-Co pre-treated cells to 15.63%±0.63 early apoptosis in Co pre-treated cells. These results are in agreement with the cell viability results where an enhanced cytotoxic effect was observed in Co pre-treated cells, and thus suggest an important role of Co ions in the metal debris toxicity.

Anti-PARP recognizes Poly-ADP-Ribose-Polymerase (PARP), a 113kD protein that binds specifically at DNA strand breaks (33). PARP is also a substrate for certain caspases (for example, caspase 3 and 7) activated during early stages of apoptosis (34). These proteases cleave PARP to fragments of approximately 89kD and 24kD and detection of one or both fragments has been used as a hallmark of apoptosis (35). Western blot analysis validated the flow cytometry results by showing the fragmentation of PARP after 48h of exposure to 2.5mg debris/1x10^6cells and 2.5mg debris/1x10^6cells with 0.1µM Co (Figure 4), which was not seen at the 24h time point. The histograms of mean optical densities for full length PARP (Figure 5), showed a significant increase, compared to controls, in the amount of PARP detected for Co pre-treated cells treated with the combination of metal debris and Co ions for 24h. Furthermore, after 48h of treatment, there was a significant decrease, compared to controls, in the amount of full length PARP detected for cells incubated in the presence of metal debris. Such a decrease in full length PARP corresponds to the fragmentation of the protein, as detected in the gels by the presence of the cleaved 89kD band, and is indicative of apoptosis.

Gene expression analysis

The StellARray™ Gene Expression System (Lonza; Switzerland) is a quantitative polymerase chain reaction (qPCR)-based method and provides profiling of biologically focused gene sets. Gene expression array analysis with the standard Human General Toxicology 96 StellARray™ was performed in order to identify genes related to the toxic effects of metal wear debris and ions on U937 cells. Cells were exposed to the combination of 2.5mg/1x10^6cells wear debris and 0.1µM Co for 120h. Untreated resting U937 cells were used as control (data not shown). Based on the results from this assay, the genes lymphotoxin

alpha (LTA), BCL2-associated athanogene (BAG1), growth arrest and DNA-damage-inducible alpha (GADD45A), inducible nitric oxide synthase (NOS2) and FBJ murine osteosarcoma viral oncogene homolog (FOS) were selected to be analysed in the context of prosthetic wear debris. Additionally, the StellARray gene set was submitted to Toppgene (36) for analysis and the chosen genes were found to be involved in at least one of the following biological processes: regulation of cell death, regulation of programmed cell death, response to toxin, negative regulation of growth, response to metal ions, regulation of cell proliferation, nitric oxide metabolic process, and oxygen and reactive oxygen species metabolic process.

To address the effect of wear particles, the mRNA expression of general human toxicology-related genes NOS2, LTA, BAG1, GADD45A, and FOS was studied 120h after treatment with 2.5mg debris/1x10^6cells, 0.1µM Co and 2.5mg debris/1x10^6cells plus 0.1µM Co (Table 5) The 120h time point was chosen to investigate the longer term effects on gene expression taking into consideration prolonged exposure to the debris in patients *in vivo*. BAG1 and NOS2 were affected by all the treatments. BAG1 expression significantly increased in cells under all treatments but was higher in the presence of Co. Expression of NOS2 decreased in the presence of metal particles but the opposite effect was observed in the presence of Co. FOS expression increased in the presence of metal debris. LTA and GADD45A were the genes less affected. Expression of LTA increased significantly in the presence of both debris and Co when cells were pre-treated with Co. Although GADD45A expression increased in cells exposed to debris, a larger effect was observed when Co pre-treated cells were exposed to both debris and Co. In general, pre-treatment with Co resulted in bigger fold changes.

Discussion

The progressive loss of bone adjacent to an implant has been attributed to a granulomatous inflammatory reaction induced by particulate implant wear debris at the bone–implant interface (37). Degradation products of metallic biomaterials include particulate wear debris, free metallic ions and inorganic metal salts or oxides (5). These are released into surrounding tissue by various mechanisms, including corrosion, wear, and mechanically accelerated electrochemical processes such as stress corrosion, corrosion fatigue, and fretting corrosion (38).

Corrosion is a natural phenomenon where higher energy states of a metal attain equilibrium by transforming to such constituents as natural ore, which have lower energy states (39). All metals in contact with a biological system undergo corrosion through an electrochemical redox reaction and an oxide layer is quickly formed on the surface of a metallic implant (40). When CoCr alloy is in contact with body fluids, cobalt is completely dissolved, and the surface oxide changes into chromium oxide containing a small amount of molybdenum oxide (41). It has been reported that local acidification may develop during acute and chronic inflammation (31). In turn, such an acidic environment, created by actively metabolizing immune cells, may enhance the corrosion process, and disrupt the surface oxide film leading to a significant increase in ions released (40). In this study, ICP-MS analysis showed significantly higher concentrations of Co and Cr when incubating wear debris at low pH. These findings suggest that the osteolysis process generated by wear debris may be exacerbated by the lowering of pH at the inflammation site, which would be in line with reports of synovial-fluid acidosis correlating with radiological joint destruction in rheumatoid-arthritis knee joints (42). Moreover, increasing ion concentrations were measured in culture medium with increasing amounts of wear debris. Results showed higher concentrations of Co than Cr, which could be explained partly by the alloy composition (62–67% Co, 27–30% Cr, 5–7 % Mo, and ~1% Ni (30)) but also by the fact that cobalt is preferentially released from CoCr alloy during the corrosion process (41). These observations seem to also be in accordance with the study carried out by Hart et al. (2012) (43). They examined periprosthetic tissue from patients with MoM hip implants and their results suggest that the amount of Co rather than its speciation is the reason for a higher failure rate. Caicedo et al. (2013) found that irregularly shaped particles have a greater surface area compared to the smooth surface of round particles and thus demonstrated a greater release of metal ions (44). In this study, SEM characterisation of the heat treated debris showed irregularly shaped particles which could have contributed to the ion release.

Molecular details of cobalt uptake are not well known and whether Co enters mammalian cells via a specific transporter is not known either (45, 46). However, it is likely that it is transported into the cells by broad-specificity divalent metal transporters (45). It has been shown that P2X7, a transmembrane ionotropic receptor, is involved in the uptake of divalent cations and Co (47). In the same way, a protein named divalent metal transporter 1 (DMT1) has been shown to have a broad substrate specificity favouring divalent metals including Co^{2+} (48). Additionally, it has been suggested that the cellular uptake of Co was mediated by

active transport ion pumps (i.e. $Ca^{2+/}Mg^{2+}$ ATPase and the Na^{+}/K^{+} ATPase) and endocytosis (49). The only biological known function of cobalt is its integral part of vitamin B12, which is incorporated into enzymes that participate in reactions essential to DNA synthesis, fatty acid synthesis and energy production (45, 46). Even though cobalt has a role in biological systems, overexposure results in toxicity due to excess (45), which promotes the development of hypoxia and increases in the level of reactive oxygen species (ROS), suppresses synthesis of ATP, initiates apoptotic and necrotic cell death (50). Cobalt ions can directly induce DNA damage, interfere with DNA repair, DNA–protein crosslinking and sister chromatid exchange (51). The exact mechanism for cobalt carcinogenicity remains to be elucidated but it has been established that cobalt-mediated free radical generation contributes to the toxicity and carcinogenicity of cobalt (52). At low doses below the no-observed-adverse-effect level (NOAEL), previous investigators have documented evidence that some nanoparticles can initiate hormesis (53). Hormesis is a dose-response relationship characterized by a low-dose stimulation and a high-dose inhibition. In the current study, the effects observed in viability could be related to such phenomenon. The 0.1µM Co concentration used in this study is very low compared to the concentrations of ions being released into the culture medium by the debris. Thus, it is possible that low concentrations of Co ions may exert an adaptive response leading to hormesis.

It has been shown that cell membranes are relatively impermeable to Cr^{3+} and the cellular uptake of Cr^{6+} is several fold greater than that of Cr^{3+} ion (54). In contrast to Cr^{3+}, Cr^{6+} is rapidly taken up by erythrocytes after absorption and reduced to Cr^{3+} inside the cell. Cr^{6+} enters the cell through non-specific anionic channels, such as the phosphate and sulphate anion exchange pathway (55). Once within the cell, Cr^{6+} is reduced metabolically by redox systems to the short-lived intermediates Cr^{5+} and Cr^{4+}, and ultimately to the most stable species, Cr^{3+} (56). Cr^{3+} interacts and forms complexes with DNA, protein and lipids resulting in increased chromium intracellular levels (55). This would also explain the higher cellular up-take of metal ions at higher debris concentrations. Cellular Co and Cr up-take results are also in agreement with previous reports of Co^{2+} having a higher capacity, in the context of implants, to penetrate cells than Cr^{3+} (57). Using microfocus X-ray spectroscopy, Hart et al. found that Co in peri-implant tissues is complexed to an organic molecule whereas Cr forms an inorganic complex with phosphate (43). Based on these findings they postulated that the materials released from the implants are not predominantly resident in the tissues as alloy particles, but as dissolved constituents of alloy particles. Furthermore, the lysosome is the

most common intracellular compartment for particles sequestration and degradation. The role of lysosomes in particles intracellular dissolution has been shown in the case of carcinogenic nickel particulate compounds (58), zinc oxide nanoparticles (59), and iron oxide microparticles (60). In this context, intracellular particle solubilisation may also contribute to the ion levels measured in this study, and could be in part responsible for the toxicity observed.

Several investigations about the effects of different kinds of metals, particles, and ions on human monocytes and macrophages have been published. Dalal et al. (61) compared the responses of human osteoblasts, fibroblasts, and macrophages exposed to particles of different metal-based particles (i.e., cobalt-chromium (CoCr) alloy, titanium (Ti) alloy, zirconium (Zr) oxide, and Zr alloy). They found that CoCr-alloy particles were by far the most toxic and decreased viability and proliferation of human osteoblasts, fibroblasts, and macrophages. Potnis et al. (62) challenged monocytes (THP-1) with Co-alloy particles and demonstrated that these particles trigger an immune response via the TLR4-MyD88-dependent pathway. Caicedo et al. (44) also challenged THP-1 cells with CoCr nanoparticles. They showed that as metal particles decrease in size, the greater the contribution of metal ions to the overall induction of IL-1β mediated responses. The release of corrosion products from implanted metals, mainly chromium, cobalt, nickel and titanium, has been associated with clinical complications such as adverse tissue reactions, promotion of infection and metal sensitivity *in vivo* as well as apoptosis and necrosis *in vitro.* (63). In the present study, apoptosis was detectable after 24h of exposure to wear debris, and wear debris combined with Co ions, and became significant after 48h as seen in both FACS and western blot analysis. Co ions on their own did not induce apoptosis probably due to low concentration (0.1µM Co). The apoptotic effects of Co ions have mainly been reported at concentrations starting from 100µM, where Co induced cell death in a dose and time dependent manner (64). Results reported herein support these observations. This suggests that the increase in ion release *in vivo* at an acidic peri-implant environment would enhance cell death and intensify the immune reaction. Several cellular components functioning in apoptosis have been reported. Among them, Bcl-2 is known to suppress multiple forms of apoptosis (65). It has been shown that co-expression of BAG1 (Bcl-2 association athagogene 1) and Bcl-2 increases protection from cell death (66). BAG1 is a multifunctional and anti-apoptotic protein that enhances the anti-apoptotic function of Bcl-2 (67). In the present study, up-regulation of BAG1 was observed in treated U937 cells compared to controls, which suggests

the cells were under apoptotic stimuli. This, in turn, suggests that BAG1 could be part of a defence mechanism for delaying cell death in response to metal toxicity, particularly Co toxicity in this case. Considering that the up-regulation was predominantly observed in the presence of Co ions treatment compared to the debris alone, cobalt could be considered a potent apoptotic inducer. The clear identification of PARP fragments at 48h complements the FACS results, which show the role of metal ions and debris as inducers of apoptosis particularly in cells that have been pre-exposed to Co^{2+}. This could have great significance for patients with failed MoM articulations undergoing revision surgery. It has been reported that at greater than one year post-removal of a large diameter MoM hip implant for the indication of symptomatic metallosis, metal ion levels in whole blood fall to almost normal levels (68). Similarly, it has been shown that serum levels of Co and Cr decrease after MoM articulation revision surgery (69). Whole blood Co and Cr ion levels before revision surgery of 18.11µg/l and 10.64µg/l, respectively; and after revision surgery of 0.39µg/l and 3.50 µg/l, respectively, have been reported (68). Similarly, average serum Co and Cr ion levels before revision surgery of 56.3µg/l and 20.5µg/l, respectively; and after revision surgery of 5.63µg/l and 2.02µg/l, respectively, have also been reported (70). The 9th National Joint Registry for England and Wales reported a total of 80,314 hip procedures performed in 2011, an increase of 5% over 2010. Of these, 8641 were revision procedures and 466 were bilateral. However, the number of patients with bilateral hip replacements is likely to be greatly underestimated since bilateral procedures are only counted as a bilateral if they are entered under the same operation during data entry. If the two procedures are recorded under two different operations they will be counted as two unilateral procedures (71). Results from this study suggest that if a second (either bilateral or revision) CoCr implant were implanted it may be more likely to produce adverse effects than the first one.

The acidic environment of inflammatory lesions is due to increased metabolic acid generation during cell activation (72). In most cases, acidosis occurs along with nitric oxide (NO) generation. In inflammatory processes, macrophages release cytokines that cause the expression of NOS2, responsible for high output production of NO for extended time periods (72). NO has been proposed to exhibit a pro-inflammatory action by enhancing NF-κB activation in response to inflammatory agents (23). qRT-PCR results analysis showed significant up-regulation of NOS2 in cells exposed to Co ions or the combination of Co ions and debris, especially in cells pre-treated with Co. Since the induction of NOS2 is characteristic of activated macrophages, these findings suggest that metal debris and ions

have the potential to activate resting macrophages. Moreover, such over-expression of NOS2 could have a predominant role in the inflammation and acidification of the peri-implant microenvironment discussed above. Additionally, NO acts in a paracrine fashion and in macrophages activates the cyclooxygenase enzyme resulting in PGE2 release. PGE2 is capable of stimulating bone resorption and is recognized as a key inflammatory mediator in wear debris–mediated peri-prosthetic bone loss (73).

Possible adverse health effects caused by accumulated metal particles in the periprosthetic tissues include osteolysis (74), inflammation, pain, and pseudotumours (75). Case et al. (76) reported that the accumulation of metal particles in lymph nodes cause structural changes such as necrosis and slight fibrosis. Additionally, there are case reports which suggest neuro- and cardio- toxicity from disseminated metal debris (15). Multiple reports (15, 16, 77-82) have described patients with MoM implants who presented systemic symptoms including neurological symptoms such as auditory impairment/deafness, visual impairment/blindness, peripheral neuropathy/dysesthesia of the extremities, poor concentration/cognitive decline, cardiomyopathy and hypothyroidism. All patients had elevated cobalt and/or chromium concentrations in their blood, serum, plasma, and/or urine, suggesting that these systemic symptoms may be due to metal toxicity as a result of excessive implant wear. Consistent with this notion, revision surgery to remove the defective metal hip prostheses resulted in lowered blood concentrations of metal ions and improved symptoms. Thus, it seems reasonable to think that systemic elevated concentrations of Co ions, due to the presence of wear debris, pose a health risk for patients bearing CoCr MoM implants.

Willert et al. (8) studied a group of patients who had a total MoM hip replacement and had early recurrence of preoperative symptoms. After revision surgery to resolve these, hip and thigh pain persisted in the patients who had received a second MoM articulation, but was alleviated where patients received revision to either a ceramic-on-polyethylene or metal-on-polyethylene bearings. The authors suggested that an immunological response persisted after the first revision and that the patients had been sensitized to the components of the all-metal articulation. The current study has found that CoCr wear metal debris may be more toxic in the presence of Co ion pre-treatment. It would be of interest to investigate the biological responses to metal wear debris of primary cells isolated from revision surgery patients at different follow-up periods. Results from this investigation also suggested that ions released from wear metal debris play an important role in the cellular response at the peri-implant

tissues. In particular, they suggested that the toxicity of Co ions could be related to nitric oxide metabolic processes and apoptosis. In conclusion, this study showed that CoCr wear debris could be more effective as an inducer of apoptosis and gene expression when cells had been pre-treated with Co ions. Results from this approach suggest that if a patient receives a second CoCr implant (revision of a MoM or a bilateral implant) it may be more likely to produce adverse effects than the first one. Consequently, this could potentially be partly responsible for the results from revision surgery being regarded as inferior to primary hip arthoplasty in terms of both function and survival (83). Priming cells with Co ions for subsequent challenge with wear debris is a novel approach within this field and could be implemented as a cell culture model for analysis of the cellular effects of metal ions and particles.

Acknowledgments

This study was supported by an Overseas Research Studentship awarded to Olga M. Posada, and by funds from University of Strathclyde. The authors are grateful to Dr C Hardaker (DePuy International) who prepared the CoCr nanoparticles.

Conflict of Interest Statement

None

References

1. Sethi RK, Neavyn MJ, Rubash HE, Shanbhag AS. Macrophage response to cross-linked and conventional UHMWPE. Biomaterials. 2003 Jul;24(15):2561-73. PubMed PMID: WOS:000182790900001. English.
2. Shimizu S, Okuda N, Kato N, Rittling SR, Okawa A, Shinomiya K, et al. Osteopontin Deficiency Impairs Wear Debris-Induced Osteolysis via Regulation of Cytokine Secretion From Murine Macrophages. Arthritis and Rheumatism. 2010 May;62(5):1329-37. PubMed PMID: WOS:000279432400016. English.
3. Liao YF, Hoffman E, Wimmer M, Fischer A, Jacobs J, Marks L. CoCrMo metal-on-metal hip replacements. Physical Chemistry Chemical Physics. 2013;15(3):746-56. PubMed PMID: WOS:000312217200002. English.
4. Zhang K, Jia TH, McQueen D, Gong WM, Markel DC, Wooley PH, et al. Circulating blood monocytes traffic to and participate in the periprosthetic tissue inflammation. Inflamm Res. 2009 Dec;58(12):837-44. PubMed PMID: WOS:000271502500002. English.
5. Hallab N, Merritt K, Jacobs JJ. Metal sensitivity in patients with orthopaedic implants. Journal of Bone and Joint Surgery-American Volume. 2001 Mar;83A(3):428-36. PubMed PMID: WOS:000167503500017.
6. Fors R, Stenberg B, Stenlund H, Persson M. Nickel allergy in relation to piercing and orthodontic appliances - a population study. Contact Dermatitis. 2012 Dec;67(6):342-50. PubMed PMID: WOS:000311056000004. English.

7. Frigerio E, Pigatto PD, Guzzi G, Altomare G. Metal sensitivity in patients with orthopaedic implants: a prospective study. Contact Dermatitis. 2011 2011;64(5):273-9. PubMed PMID: WOS:000289474000004.
8. Willert HG, Buchhorn GH, Fayyazi A, Flury R, Windler M, Koster G, et al. Metal-on-metal bearings and hypersensitivity in patients with artificial hip joints - A clinical and histomorphological study. Journal of Bone and Joint Surgery-American Volume. 2005 Jan;87A(1). PubMed PMID: WOS:000226315900006.
9. Friesenbichler J, Maurer-Ertl W, Sadoghi P, Lovse T, Windhager R, Leithner A. Serum metal ion levels after rotating-hinge knee arthroplasty: comparison between a standard device and a megaprosthesis. International Orthopaedics. 2012 Mar;36(3):539-44. PubMed PMID: WOS:000302172300010. English.
10. Penny JO, Varmarken JE, Ovesen O, Nielsen C, Overgaard S. Metal ion levels and lymphocyte counts: ASR hip resurfacing prosthesis vs. standard THA 2-year results from a randomized study. Acta Orthopaedica. 2013 Apr;84(2):130-7. PubMed PMID: WOS:000317661500003. English.
11. Simonsen LO, Harbak H, Bennekou P. Cobalt metabolism and toxicology-A brief update. The Science of the total environment. 2012 2012 Aug 15 (Epub 2012 Jun;432:210-5. PubMed PMID: MEDLINE:22732165. English.
12. Catelas I, Petit A, Vali H, Fragiskatos C, Meilleur R, Zukor DJ, et al. Quantitative analysis of macrophage apoptosis vs. necrosis induced by cobalt and chromium ions in vitro. Biomaterials. 2005 May;26(15):2441-53. PubMed PMID: WOS:000226698400027. English.
13. Xia ZD, Kwon YM, Mehmood S, Downing C, Jurkschat K, Murray DW. Characterization of metal-wear nanoparticles in pseudotumor following metal-on-metal hip resurfacing. Nanomedicine-Nanotechnology Biology and Medicine. 2011 Dec;7(6):674-81. PubMed PMID: WOS:000297699900002. English.
14. Afolaranmi GA, Akbar M, Brewer J, Grant MH. Distribution of metal released from cobalt-chromium alloy orthopaedic wear particles implanted into air pouches in mice. Journal of Biomedical Materials Research Part A. 2012 Jun;100A(6):1529-38. PubMed PMID: WOS:000302610800017.
15. Tower SS. Arthroprosthetic Cobaltism: Neurological and Cardiac Manifestations in Two Patients with Metal-on-Metal Arthroplasty A Case Report. Journal of Bone and Joint Surgery-American Volume. 2010 Dec 1;92A(17):2847-51. PubMed PMID: WOS:000285118500011.
16. Oldenburg M, Wegner R, Baur X. Severe Cobalt Intoxication Due to Prosthesis Wear in Repeated Total Hip Arthroplasty. The Journal of arthroplasty. 2009;24(5):825.e15-20.
17. Gilbert CJ, Cheung A, Butany J, Zywiel MG, Syed K, McDonald M, et al. Hip Pain and Heart Failure: The Missing Link. Canadian Journal of Cardiology. 2013 May;29(5). PubMed PMID: WOS:000318972100020.
18. Kagi D, Ho A, Odermatt B, Zakarian A, Ohashi PS, Mak TW. TNF receptor 1-dependent beta cell toxicity as an effector pathway in autoimmune diabetes. Journal of Immunology. 1999 Apr 15;162(8):4598-605. PubMed PMID: WOS:000079612100030.
19. Aveic S, Pigazzi M, Basso G. BAG1: The Guardian of Anti-Apoptotic Proteins in Acute Myeloid Leukemia. Plos One. 2011 Oct 10;6(10). PubMed PMID: WOS:000295971700039.
20. Siafakas AR, Richardson DR. Growth arrest and DNA damage-45 alpha (GADD45 alpha). International Journal of Biochemistry & Cell Biology. 2009 May;41(5):986-9. PubMed PMID: WOS:000264045000005.
21. Chen X, Zhu G, Jin T, Gu S, Xiao H, Qiu J. Cadmium induces differentiation of RAW264.7 cells into osteoclasts in the presence of RANKL. Food and Chemical Toxicology. 2011 Sep;49(9):2392-7. PubMed PMID: WOS:000295188600066.

22. Chambellan A, Leahy R, Xu W, Cruickshank PJ, Janocha A, Szabo K, et al. Pivotal role of c-Fos in nitric oxide synthase 2 expression in airway epithelial cells. Nitric Oxide-Biology and Chemistry. 2009 Apr 15;20(3):143-9. PubMed PMID: WOS:000264654200002.
23. Zeidler PC, Castranova V. Role of nitric oxide in pathological responses of the lung to exposure to environmental/occupational agents. Redox Report. 2004 2004;9(1):7-18. PubMed PMID: WOS:000220505700002.
24. Akbar M, Fraser AR, Graham GJ, Brewer JM, Grant MH. Acute inflammatory response to cobalt chromium orthopaedic wear debris in a rodent air-pouch model. Journal of the Royal Society Interface. 2012 Sep;9(74):2109-19. PubMed PMID: WOS:000306750500008. English.
25. Lutz MB, Kukutsch N, Ogilvie ALJ, Rossner S, Koch F, Romani N, et al. An advanced culture method for generating large quantities of highly pure dendritic cells from mouse bone marrow. Journal of Immunological Methods. 1999 Feb 1;223(1):77-92. PubMed PMID: WOS:000078463300007.
26. Lowry OH, Rosebrough NJ, Farr AL, Randall RJ. Protein measurement with the folin phenol reagent. Journal of Biological Chemistry. 1951 1951;193(1):265-75. PubMed PMID: WOS:A1951UC36200032.
27. Ye J, Coulouris G, Zaretskaya I, Cutcutache I, Rozen S, Madden TL. Primer-BLAST: A tool to design target-specific primers for polymerase chain reaction. Bmc Bioinformatics. 2012 Jun 18;13. PubMed PMID: WOS:000307215100001.
28. Livak KJ, Schmittgen TD. Analysis of relative gene expression data using real-time quantitative PCR and the 2(T)(-Delta Delta C) method. Methods. 2001 Dec;25(4):402-8. PubMed PMID: WOS:000173949500003.
29. Xie F, Xiao P, Chen D, Xu L, Zhang B. miRDeepFinder: a miRNA analysis tool for deep sequencing of plant small RNAs. Plant Molecular Biology. 2012 Sep;80(1):75-84. PubMed PMID: WOS:000307539800007.
30. Singh R, Dahotre NB. Corrosion degradation and prevention by surface modification of biometallic materials. Journal of Materials Science-Materials in Medicine. 2007 May;18(5). PubMed PMID: WOS:000246564200008.
31. Rajamaki K, Nordstrom T, Nurmi K, Akerman KEO, Kovanen PT, Oorni K, et al. Extracellular Acidosis Is a Novel Danger Signal Alerting Innate Immunity via the NLRP3 Inflammasome. Journal of Biological Chemistry. 2013 May;288(19):13410-9. PubMed PMID: CCC:000318850300026. English.
32. Ortega R, Bresson C, Darolles C, Gautier C, Roudeau S, Perrin L, et al. Low-solubility particles and a Trojan-horse type mechanism of toxicity: the case of cobalt oxide on human lung cells. Particle and fibre toxicology. 2014 2014;11(1):14. PubMed PMID: MEDLINE:24669904. English.
33. Demurcia G, Demurcia JM. Poly(adp-ribose) polymerase - a molecular nick-sensor. Trends in Biochemical Sciences. 1994 Apr;19(4):172-6. PubMed PMID: WOS:A1994NG58800009.
34. Nicholson DW, Ali A, Thornberry NA, Vaillancourt JP, Ding CK, Gallant M, et al. Identification and inhibition of the ice/ced-3 protease necessary for mammalian apoptosis. Nature. 1995 Jul 6;376(6535):37-43. PubMed PMID: WOS:A1995RH11100055.
35. Gambi N, Tramontano F, Quesada P. Poly(ADPR)potymerase inhibition and apoptosis induction in cDDP-treated human carcinoma cell lines. Biochemical Pharmacology. 2008 Jun 15;75(12):2356-63. PubMed PMID: WOS:000257257400010.
36. Chen J, Bardes EE, Aronow BJ, Jegga AG. ToppGene Suite for gene list enrichment analysis and candidate gene prioritization. Nucleic Acids Research. 2009 Jul 1;37:W305-W11. PubMed PMID: WOS:000267889100054.

37. Vasudevan A, DiCarlo EF, Wright T, Chen D, Figgie MP, Goldring SR, et al. Cellular Response to Prosthetic Wear Debris Differs in Patients With and Without Rheumatoid Arthritis. Arthritis and Rheumatism. 2012 Apr;64(4):1005-14. PubMed PMID: WOS:000302475500009. English.
38. Okazaki Y, Gotoh E. Comparison of metal release from various metallic biomaterials in vitro. Biomaterials. 2005 Jan;26(1):11-21. PubMed PMID: WOS:000223948200002.
39. Sargeant A, Goswami T. Hip implants - Paper VI - Ion concentrations. Materials & Design. 2007 2007;28(1):155-71. PubMed PMID: WOS:000242785600018.
40. Cadosch D, Al-Mushaiqri MS, Gautschi OP, Meagher J, Simmen H-P, Filgueira L. Biocorrosion and uptake of titanium by human osteoclasts. Journal of Biomedical Materials Research Part A. 2010 Dec 15;95A(4):1004-10. PubMed PMID: WOS:000284023200004.
41. Hanawa T. Metal ion release from metal implants. Materials Science & Engineering C-Biomimetic and Supramolecular Systems. 2004 Dec 1;24(6-8):745-52. PubMed PMID: WOS:000225498200008.
42. Mansson B, Geborek P, Saxne T, Bjornsson S. Cytidine deaminase activity in synovial-fluid of patients with rheumatoid-arthritis - relation to lactoferrin, acidosis, and cartilage proteoglycan release. Annals of the Rheumatic Diseases. 1990 Aug;49(8):594-7. PubMed PMID: WOS:A1990DQ03500006.
43. Hart AJ, Quinn PD, Lali F, Sampson B, Skinner JA, Powell JJ, et al. Cobalt from metal-on-metal hip replacements may be the clinically relevant active agent responsible for periprosthetic tissue reactions. Acta Biomaterialia. 2012 Oct;8(10):3865-73. PubMed PMID: WOS:000309301400033. English.
44. Caicedo MS, Samelko L, McAllister K, Jacobs JJ, Hallab NJ. Increasing both CoCrMo-alloy particle size and surface irregularity induces increased macrophage inflammasome activation in vitro potentially through lysosomal destabilization mechanisms. Journal of Orthopaedic Research. 2013 Oct;31(10):1633-42. PubMed PMID: WOS:000323305000019.
45. Bleackley MR, MacGillivray RTA. Transition metal homeostasis: from yeast to human disease. Biometals. 2011 Oct;24(5):785-809. PubMed PMID: WOS:000294463300002. English.
46. Catalani S, Rizzetti MC, Padovani A, Apostoli P. Neurotoxicity of cobalt. Human & Experimental Toxicology. 2012 May;31(5):421-37. PubMed PMID: WOS:000303552400001. English.
47. Virginio C, Church D, North RA, Surprenant A. Effects of divalent cations, protons and calmidazolium at the rat P2X(7) receptor. Neuropharmacology. 1997 Sep;36(9):1285-94. PubMed PMID: WOS:A1997YD89200016.
48. Griffin KP, Ward DT, Liu W, Stewart G, Morris ID, Smith CP. Differential expression of divalent metal transporter DMT1 (Slc11a2) in the spermatogenic epithelium of the developing and adult rat testis. American Journal of Physiology-Cell Physiology. 2005 Jan;288(1):C176-C84. PubMed PMID: WOS:000225640900019.
49. Kasten U, Hartwig A, Beyersmann D. Mechanisms of cobalt(II) uptake into v79-chinese hamster-cells. Archives of Toxicology. 1992 Oct;66(8):592-7. PubMed PMID: WOS:A1992JU01700010.
50. Kravenskaya YV, Fedirko NV. Mechanisms Underlying Interaction of Zinc, Lead, and Cobalt with Nonspecific Permeability Pores in the Mitochondrial Membranes. Neurophysiology. 2011 Nov;43(3):163-72. PubMed PMID: WOS:000297624700001. English.
51. Valko M, Morris H, Cronin MTD. Metals, toxicity and oxidative stress. Current Medicinal Chemistry. 2005 2005;12(10). PubMed PMID: WOS:000228824700003.

52. De Boeck M, Kirsch-Volders M, Lison D. Cobalt and antimony: genotoxicity and carcinogenicity. Mutation Research-Fundamental and Molecular Mechanisms of Mutagenesis. 2003 Dec 10;533(1-2). PubMed PMID: WOS:000208033800008.
53. Nascarella MA, Calabrese EJ. A method to evaluate hormesis in nanoparticle dose-responses. Dose-Response. 2012 2012;10(3):344-54. PubMed PMID: WOS:000307836500004.
54. Biedermann KA, Landolph JR. Role of valence state and solubility of chromium compounds on induction of cytotoxicity, mutagenesis, and anchorage independence in diploid human fibroblastS. Cancer Research. 1990 Dec 15;50(24):7835-42. PubMed PMID: WOS:A1990EM16500020.
55. Raja NS, Sankaranarayanan K, Dhathathreyan A, Nair BU. Interaction of chromium(III) complexes with model lipid bilayers: Implications on cellular uptake. Biochimica Et Biophysica Acta-Biomembranes. 2011 Jan;1808(1):332-40. PubMed PMID: WOS:000285853800036.
56. Afolaranmi GA, Tettey J, Meek RMD, Grant MH. Release of chromium from orthopaedic arthroplasties. The open orthopaedics journal. 2008 2008 Jan;2:10-8. PubMed PMID: MEDLINE:19461924.
57. Catelas I, Petit A, Zukor DJ, Huk OL. Cytotoxic and apoptotic effects of cobalt and chromium ions on J774 macrophages - Implication of caspase-3 in the apoptotic pathway. Journal of Materials Science-Materials in Medicine. 2001;12(10-12):949-53. PubMed PMID: WOS:000172280300020. English.
58. Munoz A, Costa M. Elucidating the mechanisms of nickel compound uptake: A review of particulate and nano-nickel endocytosis and toxicity. Toxicology and Applied Pharmacology. 2012 Apr 1;260(1):1-16. PubMed PMID: WOS:000302253800001.
59. Cho W-S, Duffin R, Howie SEM, Scotton CJ, Wallace WAH, MacNee W, et al. Progressive severe lung injury by zinc oxide nanoparticles; the role of Zn2+ dissolution inside lysosomes. Particle and Fibre Toxicology. 2011 Sep 6;8. PubMed PMID: WOS:000295375900001.
60. Beck-Speier I, Kreyling WG, Maier KL, Dayal N, Schladweiler MC, Mayer P, et al. Soluble iron modulates iron oxide particle-induced inflammatory responses via prostaglandin E-2 synthesis: In vitro and in vivo studies. Particle and Fibre Toxicology. 2009 Dec 22;6. PubMed PMID: WOS:000273814600001.
61. Dalal A, Pawar V, McAllister K, Weaver C, Hallab NJ. Orthopedic implant cobalt-alloy particles produce greater toxicity and inflammatory cytokines than titanium alloy and zirconium alloy-based particles in vitro, in human osteoblasts, fibroblasts, and macrophages. Journal of Biomedical Materials Research Part A. 2012 Aug;100A(8):2147-58. PubMed PMID: WOS:000305509700025. English.
62. Potnis PA, Dutta DK, Wood SC. Toll-like receptor 4 signaling pathway mediates proinflammatory immune response to cobalt-alloy particles Cellular Immunology. 2013;282:53-65.
63. Granchi D, Cenni E, Ciapetti G, Savarino L, Stea S, Gamberini S, et al. Cell death induced by metal ions: necrosis or apoptosis? Journal of Materials Science-Materials in Medicine. 1998 Jan;9(1):31-7. PubMed PMID: WOS:000071589400005. English.
64. Akbar M, Brewer JM, Grant MH. Effect of chromium and cobalt ions on primary human lymphocytes in vitro. J Immunotoxicol. 2011 Jun;8(2):140-9. PubMed PMID: WOS:000290167000005. English.
65. Willis S, Day CL, Hinds MG, Huang DCS. The Bcl-2-regulated apoptotic pathway. Journal of Cell Science. 2003 Oct 15;116(20):4053-6. PubMed PMID: WOS:000187395200001.

66. Terada S, Komatsu T, Fujita T, Terakawa A, Nagamune T, Takayama S, et al. Co-expression of bcl-2 and bag-1, apoptosis suppressing genes, prolonged viable culture period of hybridoma and enhanced antibody production. Cytotechnology. 1999 1999-Sep;31(1-2):143-51. PubMed PMID: MEDLINE:19003134.
67. Tang SC. BAG-1, an anti-apoptotic tumour marker. Iubmb Life. 2002 Feb;53(2):99-105. PubMed PMID: WOS:000175450300004.
68. Ebreo D, Khan A, El-Meligy M, Armstrong C, Peter V. Metal ion levels decrease after revision for metallosis arising from large-diameter metal-on-metal hip arthroplasty. Acta Orthopaedica Belgica. 2011 Dec;77(6):777-81. PubMed PMID: WOS:000298869800010. English.
69. Maezawa K, Nozawa M, Matsuda K, Sugimoto M, Shitoto K, Kurosawa H. Serum Chromium levels before and after revision surgery for loosened metal-on-metal total hip arthroplasty. journal of arthroplasty. 2009 Jun;24(4):549-53. PubMed PMID: WOS:000266846500010. English.
70. Ball ST, Severns D, Linn M, Meyer RS, Swenson FC. What happens to serum metal ion levels after a metal-on-metal bearing is removed? The Journal of arthroplasty. 2013 2013-Sep;28(8 Suppl):53-5. PubMed PMID: MEDLINE:23948123.
71. National Joint Registry N. National Joint Registry for England and Wales 9th Annual Report. www.njrcentre.org.uk. 2012.
72. Bellocq A, Suberville S, Philippe C, Bertrand F, Perez J, Fouqueray B, et al. Low environmental pH is responsible for the induction of nitric-oxide synthase in macrophages - Evidence for involvement of nuclear factor-kappa B activation. Journal of Biological Chemistry. 1998 Feb 27;273(9):5086-92. PubMed PMID: WOS:000072310400044.
73. Shanbhag AS, Macaulay W, Stefanovic-Racic M, Rubash HE. Nitric oxide release by macrophages in response to particulate wear debris. Journal of Biomedical Materials Research. 1998 Sep;41(3):497-503. PubMed PMID: WOS:000074523300021. English.
74. Huber M, Reinisch G, Zenz P, Zweymueller K, Lintner F. Postmortem study of femoral osteolysis associated with metal-on-metal articulation in total hip replacement an analysis of nine cases. Journal of Bone and Joint Surgery-American Volume. 2010 Jul 21;92A(8):1720-31. PubMed PMID: WOS:000280216600005.
75. Langton DJ, Joyce TJ, Jameson SS, Lord J, Van Orsouw M, Holland JP, et al. Adverse reaction to metal debris following hip resurfacing The influence of component type, orientation and volumetric weaR. Journal of Bone and Joint Surgery-British Volume. 2011 Feb;93B(2):164-71. PubMed PMID: WOS:000287378300005.
76. Case CP, Langkamer VG, James C, Palmer MR, Kemp AJ, Heap PF, et al. Widespread dissemination of metal debris from implants. Journal of Bone and Joint Surgery-British Volume. 1994 Sep;76B(5). PubMed PMID: WOS:A1994PH52600005.
77. Steens W, von Foerster G, Katzer A. Severe cobalt poisoning with loss of sight after ceramic-metal pairing in a hip- a case report. Acta Orthopaedica. 2006 Oct;77(5):830-2. PubMed PMID: WOS:000240954000023.
78. Ikeda T, Takahashi K, Kabata T, Sakagoshi D, Tomita K, Yamada M. Polyneuropathy caused by cobalt-chromium metallosis after total hip replacement. Muscle Nerve. 2010 Jul;42(1):140-3. PubMed PMID: WOS:000279456400020. English.
79. Machado C, Appelbe A, Wood R. Arthroprosthetic Cobaltism and Cardiomyopathy. Heart Lung and Circulation. 2012 Nov;21(11):759-60. PubMed PMID: WOS:000311775400021.
80. Pelclova D, Sklensky M, Janicek P, Lach K. Severe cobalt intoxication following hip replacement revision: Clinical features and outcome. Clinical Toxicology. 2012 Apr;50(4):262-5. PubMed PMID: WOS:000302024600006.

81. Rizzetti MC, Liberini P, Zarattini G, Catalani S, Pazzaglia U, Apostoli P, et al. Loss of sight and sound. Could it be the hip? Lancet. 2009 Mar 21;373(9668):1052-. PubMed PMID: WOS:000264398200034.
82. Tower SS. METAL ON METAL HIP IMPLANTS Arthroprosthetic cobaltism associated with metal on metal hip implants. British Medical Journal. 2012 Jan 17;344. PubMed PMID: WOS:000300041800026.
83. Dattani R, Blunn G. Revision of the femoral prosthesis with impaction allografting. Acta Orthopaedica Belgica. 2007 Oct;73(5):558-65. PubMed PMID: WOS:000254245000002.

Figure, Image and table captions

Image 1. Scanning Electron Microscopy images of simulator generated wear debris from an ASR hip implant. Images taken at B) 50kX and D) 5kX with a FE-SEM Hitachi SU-6600.

Figure 1. Metal ions in RPMI-1640 medium released from different concentrations of wear metal debris (per million cells) incubated with U937 cells for 24h. (a) Cr ion levels. (b) Co ion levels. (c) Mo ion levels. Results are expressed as mean values (±SEM, n=6). N.B. difference in *y*-axes. All values are significantly different from control (0mg debris/1x10^6cells) values ($p<0.05$) by one-way ANOVA followed by Dunnett's multiple comparison test.

Figure 2. Cellular ion up-take after 24h exposure to different concentrations of wear metal debris. Results are expressed as mean values (±SEM, n=6). All values are significantly different from control (0mg debris /1x10^6cells) values ($p<0.05$) by one-way ANOVA followed by Dunnett's multiple comparison test.

Figure 3. Early and late apoptosis of resting and Co pre-treated resting U937 cells exposed to 2.5mg debris/1x10^6cells, 0.1µM Co and a combination of 2.5mg debris/1x10^6cells and 0.1µM Co, measured by FACS. (a) Early apoptosis after 24h of treatment. (b) Late apoptosis after 24h of treatment. (c) Early apoptosis after 48h of treatment. (d) Late apoptosis after 48h of treatment. Results are mean values (±SEM, n=6). *Significantly different from control values ($p<0.05$) by one-way ANOVA followed by Dunnett's multiple comparison test. †Significant difference between non-Co pre-treated cell and Co pre-treated cell values ($p<0.05$) by Two-sample t-Test.

Figure 4. Western blot analysis of extracts from U937 and Co pre-treated U937 cells showing PARP cleavage as evidence of induction of apoptosis. (a) Full length (113kD) PARP after 24h of treatment. (b) Full length (113kD) and cleaved (89kD) PARP after 48h of treatment. Cells were exposed for 24 and 48h to 2.5mg debris/1x10^6cells, 0.1µM Co and a combination of 2.5mg debris/1x10^6cells and 0.1µM Co. Lanes: 1. Molecular weight marker, 2. Control, 3. U937+2.5mg, 4. U937+0.1µM Co, 5. U937+2.5mg+0.1µM Co, 6. Co pre-treated U937+2.5mg, 7. Co pre-treated U937+0.1µM Co, 8. Co pre-treated U937+2.5mg+0.1µM Co.

Figure 5. Optical densities of full length (113kD) PARP bands in western blot gels of extracts from U937 and Co pre-treated U937 cells exposed to 2.5mg debris/1x10^6cells, 0.1µM Co and a combination of 2.5mg debris/1x10^6cells and 0.1µM Co. (a) Full length PARP after 24h of treatment. **(b)** Full length PARP after 48h of treatment. Results are mean values (± SEM, n=3). *Significantly different from control values ($p<0.05$) by one-way ANOVA followed by Dunnett's multiple comparison test. †Significant difference between non-Co pre-treated cell and Co pre-treated cell values ($p<0.05$) by Two-sample t-Test.

Table 1. PCR Primers used for qRT-PCR gene expression analysis. Table contains the gene symbol, GenBank accession number, primer sequence, melting temperatures (Tm) and predicted amplicon size for the primer sets used in this study.

Table 2. Cell viability at 24 and 120h measured by Neutral Red and MTT. Results are percentage values (Mean ± SEM, n=9) where 100% corresponds to control values (Absorbance values 24h MTT:0.323 , NR:0.256 ; 48h MTT:0.686 , NR:0.317 ; 120h MTT:1.019, NR:0.467). *Significantly different from control values ($p<0.05$) by one-way ANOVA followed by Dunnett's multiple comparison test. †Significant difference between non-Co pre-treated cell and Co pre-treated cell values ($p<0.05$) by Two-sample t-Test.

Table 3. Metal ions in RPMI-1640 in the presence and absence of metal wear debris and no cells. Results are expressed as mean values (±SEM, n=3). *Significantly different control values ($p<0.05$) by one-way ANOVA followed by Dunnett's multiple comparison test. †Significant difference between pH 7.4 and pH 4.0.

Table 4. Cellular ion up-take after 24h exposure to different concentrations of wear metal debris. Results are expressed as mean values (±SEM, n=3). All values are significantly different from control (0mg debris /1x10^{6}cells) values ($p<0.05$) by one-way ANOVA followed by Dunnett's multiple comparison test.

Table 5. Fold variations of mRNA expression of U937 cells treated with 2.5mg debris/1x10^{6}cells, 0.1µM Co and 2.5mg debris/1x10^{6}cells plus 0.1µM Co. mRNA was analysed by real-time RT-PCR. Untreated cells were used as control. Results are normalized to HPRT1 and given as fold increase of the mRNA levels in treated cells versus controls (1). Fold variation values are given as mean ± SEM of triplicates. All values significantly increased compared to control cells ($p < 0.05$) unless otherwise noted (ns, not significant). *Significantly lower than in control cells ($p < 0.05$).

Gene	Primer sequences (5'-> 3'), (nucleotides)		Tm	Amplicon size (bp)
NOS2 NM_000625	Sense	GTGCAAACCTTCAAGGCAGCCT (22)	59.3	127
	Anti-sense	TGAGTCCTGCACGAGCCTGTAGTG (24)	60.3	
LTA NM_001159740	Sense	TGCTGCTCACCTCATTGGAGACC (23)	60.1	123
	Anti-sense	CTGGTGGGGACCAGGAGAGAATT (23)	59.2	
BAG1 NM_004323	Sense	TGCCCAAGGATTTGCAAGCTG (21)	59.7	113
	Anti-sense	TTCTGGCAGGATCAGTGTGTCAATC (25)	59.9	
GADD45A NM_001924	Sense	AACATCCTGCGCGTCAGCAAC (21)	59.7	137
	Anti-sense	AGATGAATGTGGATTCGTCACCAGC (25)	60.1	
FOS NM_005252	Sense	ACGCAGACTACGAGGCGTCATCC (23)	61.3	142
	Anti-sense	GCCAGGTCCGTGCAGAAGTCC (21)	60.4	
B2M NM_004048	Sense	AGATGAGTATGCCTGCCGTGTGAAC (25)	60.3	110
	Anti-sense	CAAATGCGGCATCTTCAAACCTC (23)	59.5	
HPRT1 NM_000194	Sense	CCCTGGCGTCGTGATTAGTGATG (23)	60.2	138
	Anti-sense	CGAGCAAGACGTTCAGTCCTGTCC (24)	60.9	
GAPDH NM_002046	Sense	AGCCTCCCGCTTCGCTCTC (20)	58.2	125
	Anti-sense	ACCAAATCCGTTGACTCCGACC (23)	58.7	

Table 1

Cell Viability 24h

Neutral Red

Cells	Treatments: 5mg debris/1x10^{6}cells	0.1µM of Co^{2+}	5mg debris/1x10^{6}cells + 0.1µM of Co^{2+}
No Co pre-treatment	99.00±7.76	96.40±10.37	79.84±3.01
Co pre-treated	77.46*†±4.72	81.53±6.67	72.04*±3.12

MTT

Cells	Treatments: 5mg debris/1x10^{6}cells	0.1µM of Co^{2+}	5mg debris/1x10^{6}cells + 0.1µM of Co^{2+}
No Co pre-treatment	125.21±11.97	161.39*±13.71	161.26*±7.06
Co pre-treated	144.63*±6.06	146.28*±11.35	117.15†±6.21

Cell Viability 48h

Neutral Red

Cells	Treatments: 5mg debris/1x10^{6}cells	0.1µM of Co^{2+}	5mg debris/1x10^{6}cells + 0.1µM of Co^{2+}
No Co pre-treatment	79.01*±6.72	89.72±3.81	71.51*±5.58
Co pre-treated	67.57*±2.46	88.78±3.18	63.53*±1.11

MTT

Cells	Treatments: 5mg debris/1x10^{6}cells	0.1µM of Co^{2+}	5mg debris/1x10^{6}cells + 0.1µM of Co^{2+}
No Co pre-treatment	65.72*±3.48	117.98±7.65	77.84*±6.21
Co pre-treated	56.65*±3.73	98.49±4.72	72.19*±3.67

Cell Viability 120h

Neutral Red

Cells	Treatments: 5mg debris/1x10^{6}cells	0.1µM of Co^{2+}	5mg debris/1x10^{6}cells + 0.1µM of Co^{2+}
No Co pre-treatment	34.68*±4.57	121.12*±5.44	57.47*±4.50
Co pre-treated	30.42*±2.59	100.12±9.85	31.84*†±4.68

MTT

Cells	Treatments: 5mg debris/1x10^{6}cells	0.1µM of Co^{2+}	5mg debris/1x10^{6}cells + 0.1µM of Co^{2+}
No Co pre-treatment	22.11*±7.78	129.70*±8.70	27.83*±6.84
Co pre-treated	11.74*±1.96	111.74±12.92	14.61*±1.57

Table 2

Condition	Mean Concentration [µg/l] ± SEM		
	Cr	Co	Mo
RPMI – FCS (control)	0.15±0.12	0.03±0.03	3.17±0.33
RPMI - FCS + Co-Cr wear debris	15.91*±1.65	1226.56*±38.97	127.82*±4.28
RPMI + 10% FCS (control)	0.19±0.06	0.09±0.09	6.32±0.16
RPMI + 10% FCS + Co-Cr wear debris	18.18*±2.64	1259.41*±39.58	124.60*±2.70
pH4 RPMI + 10% FCS + Co-Cr wear debris	372.10*†±14.45	3182.85*†±115.68	222.26*†±7.69

Table 3

Debris concentrations per $1x10^6$cells	Cr (fg/cell) Mean± SEM	Co (fg/cell) Mean± SEM
0.2mg	3.18±1.27	10.18±0.64
0.5mg	5.09±0.64	24.17±1.27
1mg	3.75±0.06	32.44±1.10
2.5mg	16.54±0.64	122.14±2.92
5mg	14.63±0.64	110.05±3.18

Table 4

Cells	Treatment	Fold Change				
		NOS2	LTA	BAG1	GADD45A	FOS
U937	2.5mg debris/1x10^{6}cells	0.36±0.03*	1.06±0.03 (ns)	2.19±0.14	1.16±0.50	2.55±0.07
	0.1µMCo	66.56±4.81	0.50±0.08(ns)	8.87±0.71	0.34±0.17(ns)	0.73±0.04(ns)
	2.5mg debris/1x10^{6}cells +0.1µMCo	75.25±26.80	0.78±0.32(ns)	22.09±4.07	0.19±0.04(ns)	1.68±0.19
Co pre-treated U937	2.5mg debris/1x10^{6}cells	0.38±0.07*	0.93±0.08(ns)	3.25±0.20	0.24±0.11(ns)	2.07±0.20
	0.1µMCo	275.89±40.51	0.73±0.09(ns)	11.56±0.39	0.57±0.19(ns)	0.82±0.12(ns)
	2.5mg debris/1x10^{6}cells +0.1µMCo	423.38±10.83	2.75±0.13	9.08±0.73	11.45±1.24	2.94±0.26

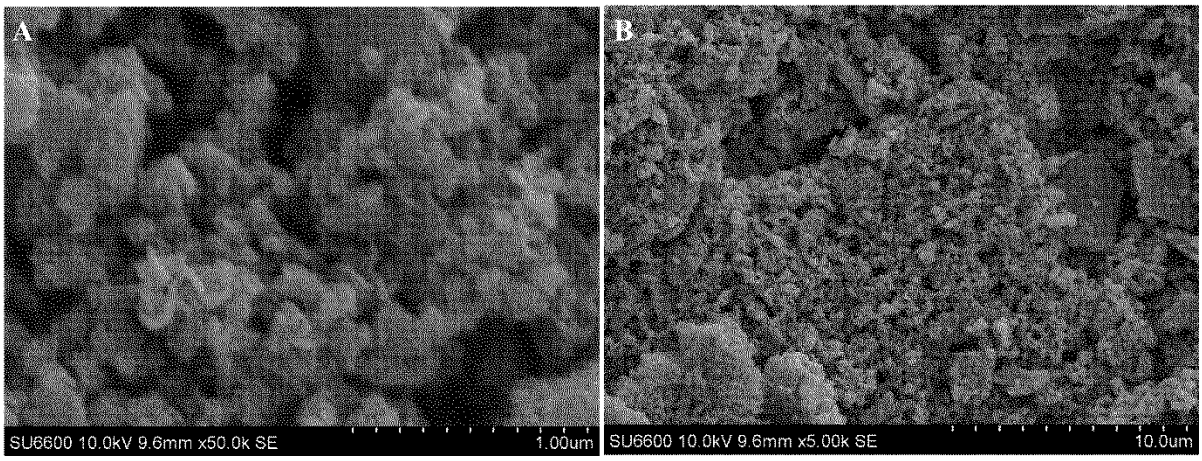
A
SU6600 10.0kV 9.6mm x50.0k SE
1.00um
B
SU6600 10.0kV 9.6mm x5.00k SE
10.0um

Image 1

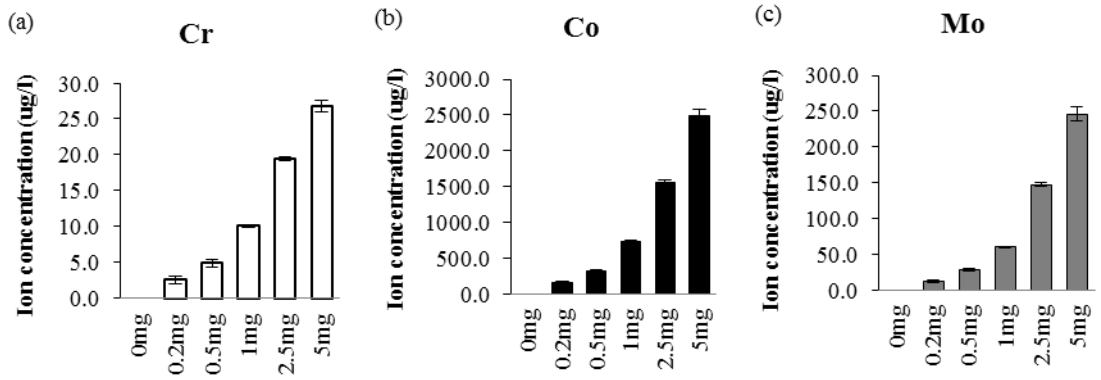
(a)
Cr
Ion concentration (ug/l)
30.0
25.0
20.0
15.0
10.0
5.0
0.0
0mg
0.2mg
0.5mg
1mg
2.5mg
5mg
(b)
Co
Ion concentration (ug/l)
3000.0
2500.0
2000.0
1500.0
1000.0
500.0
0.0
0mg
0.2mg
0.5mg
1mg
2.5mg
5mg
(c)
Mo
Ion concentration (ug/l)
300.0
250.0
200.0
150.0
100.0
50.0
0.0
0mg
0.2mg
0.5mg
1mg
2.5mg
5mg

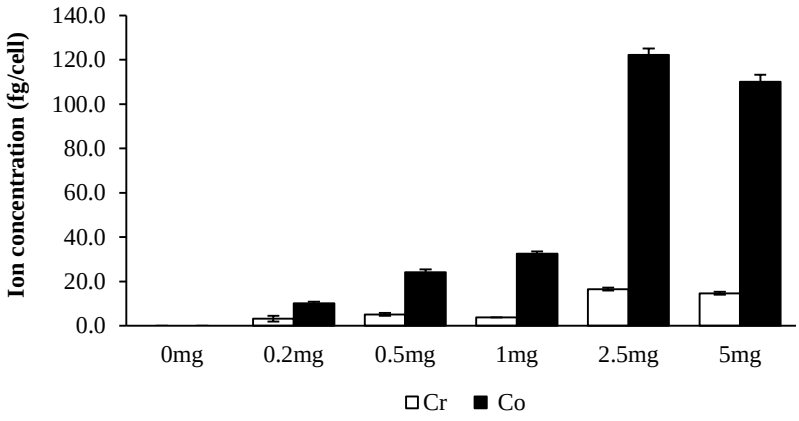
Ion concentration (fg/cell)
140.0
120.0
100.0
80.0
60.0
40.0
20.0
0.0
0mg
0.2mg
0.5mg
1mg
2.5mg
5mg
Cr
Co

Figure 2

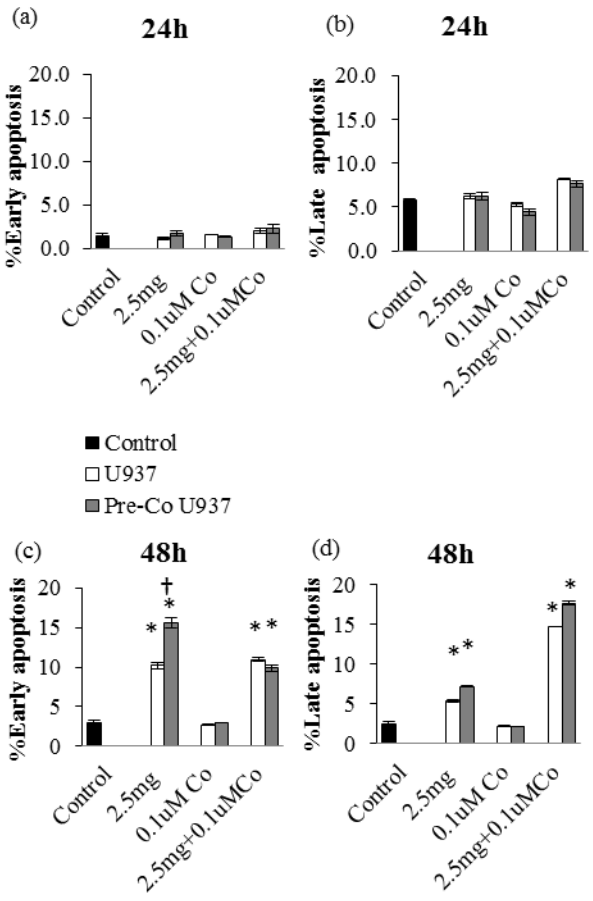
(a)
24h
%Early apoptosis
20.0
15.0
10.0
5.0
0.0
Control
2.5mg
0.1uM Co
2.5mg+0.1uMCo
(b)
24h
%Late apoptosis
20.0
15.0
10.0
5.0
0.0
Control
2.5mg
0.1uM Co
2.5mg+0.1uMCo
Control
U937
Pre-Co U937
(c)
48h
%Early apoptosis
20
15
10
5
0
†
*
*
*
*
Control
2.5mg
0.1uM Co
2.5mg+0.1uMCo
(d)
48h
%Late apoptosis
20
15
10
5
0
*
*
*
*
Control
2.5mg
0.1uM Co
2.5mg+0.1uMCo

Figure 3

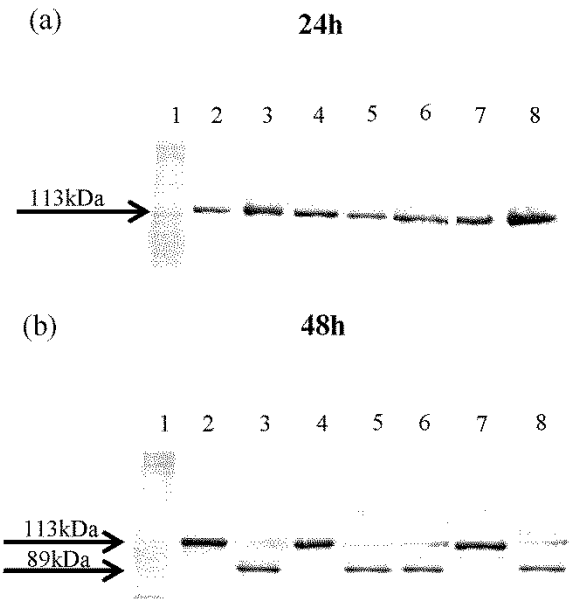

Figure 4

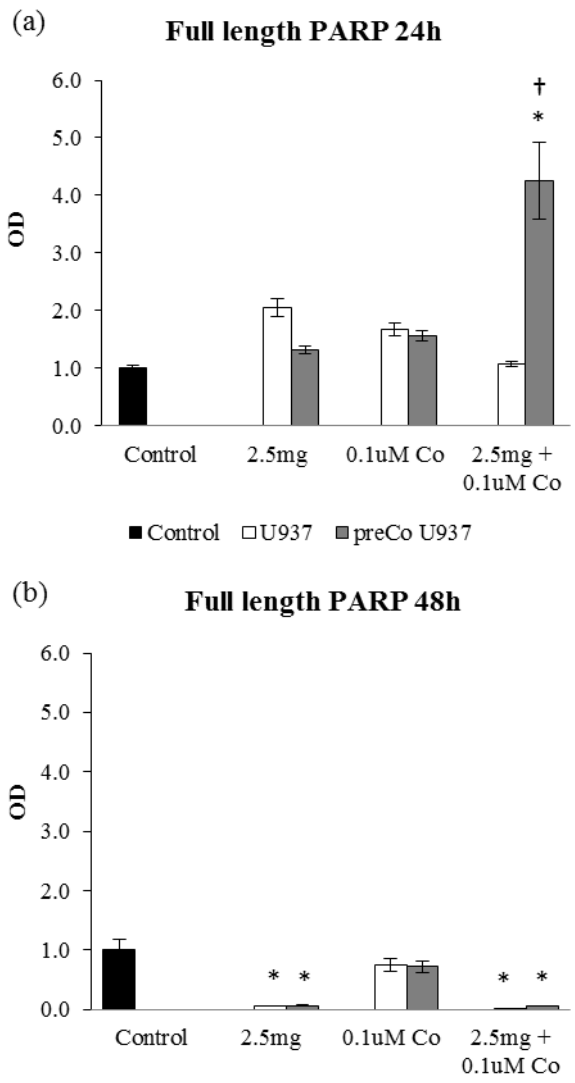
(a)
Full length PARP 24h
OD
6.0
5.0
4.0
3.0
2.0
1.0
0.0
†
*
Control
2.5mg
0.1uM Co
2.5mg + 0.1uM Co
Control
U937
preCo U937
(b)
Full length PARP 48h
OD
6.0
5.0
4.0
3.0
2.0
1.0
0.0
* *
* *
Control
2.5mg
0.1uM Co
2.5mg + 0.1uM Co

Figure 5